Journal of Applied Fluid Mechanics, Vol. 10, No. 6, pp. 1729-1745, 2017.
Available online at www.jafmonline.net, ISSN 1735-3572, EISSN 1735-3645.
DOI: 10.29252/jafm.73.245.27410

Study of Snow Accumulation on a High-Speed Train's Bogies Based on the Discrete Phase Model

F. Xie[1,2], J. Zhang[1,2], G. Gao[1,2†], K. He[1,2], Y. Zhang[1,2], J. Wang[1,2] and Y. Zhang[1,2]

[1] *Key Laboratory of Traffic Safety on Track of Ministry of Education, Changsha, Hunan 410075, China*
[2] *School of Traffic & Transportation Engineering, Central South University, Changsha, Hunan, 410075, China*

†*Corresponding Author Email: gjgao@csu.edu.cn*

(Received November 20, 2016; accepted August 8, 2017)

ABSTRACT

During winters, the high-speed train travels in the northern of China is struck by to the snow, ice and coldness, massive snow accumulating on the bogies. To understand the cause of snow packing on the high-speed train's bogies clearly, the 3-D unsteady Reynolds-averaged Navier-Stokes equations with a RNG double-equations turbulence model and a DPM discrete phase model were used to investigate the flow field carried snow particles in a single high-speed train bogie region and monitor the movement of snow particles. And, the numerical simulation was verified by the wind tunnel test. The results show that when air flows into the region, the airflow will rise and impact on the wheels, brakes, electromotors and other parts of bogie regions. The snow particles will follow the air, while the air direction changes sharply the particles will keep the movement due to the inertia. Afterwards, the snow packs on the bogie. In front of the bogies the streamlines of the air and the particle path lines are basically the same. However, due to the inertia of mass particles, the following characteristics of the snow particles with the air are not obvious in the bogie leeward side. Different structures of the end plates will affect the snow accumulation in the bogie regions.

Keywords: Bogie; Discrete phase; Snow accumulation; Flow characteristics.

NOMENCLATURE

C_D	resistance coefficient	Re	relative Reynolds number
d_p	diameter of particles	$\vec{x}$	particle displacement vector
$F_D(\vec{u}-\vec{u}_p)$	aerodynamic force	μ	dynamic viscosity
$\vec{g}$	inertia acceleration vector	ρ_p	density of particles
$\vec{u}$	fluid phase velocity vector	ρ	density of air
$\vec{u}_p$	velocity of particle phase		

1 INTRODUCTION

When the high-speed train services in a cold winter, the snow laid on the ground and ballast will whirl around the train while in motion. Although on the track there seems to be less snow, the train is surrounded by a cloud of snow. This kind of snow is composed of very fine and light particles (Kloow 2006), as shown in Fig. 1, and easily be affected by the slipstream of the train. Besides these, the snow is also easily adhered to the train, such as the bogies.

On the other hand, the harsh weather conditions related to temperature changes – the crossing of the point zero centigrade – will lead to the most destructiveness when the ice accretion build up on the train, especially on the bogies. This procedure depends on the heat sources that make the snow melt. The train running at a high speed is powered by the electromotors that is fixed on the bogies. Therefore, it would be one kind of heat sources. When the train takes emergency braking, the brakes will generate lots of heat that causes the snow to melt, so they become the second kind of heat

sources. If the train packing snow enters a warmer region, such as a long tunnel, this will be the third kind of heat sources. After that, when the train faces the cold surroundings with the degree below zero again, the problem will occur that the melted snow freezes to the ice occurs. In such circulation, snow will gradually accumulate in the area of the bogies, as shown in Fig. 2.

Fig. 1. Snow smoke produced by the tilting train of the Swedish X2.

Fig. 2. Bogies covered with snow and ice.

At the same time, when the snow accumulates on the elastic components such as the journal box spring, coil spring and air spring of the train, their vibration in the vertical direction will compress the light snow, resulting in high – density obstacles laid in the moving range. Eventually all these will deteriorate the vehicle dynamic characteristics. The worst is some systems, such as the brake system, are froze to failure, which will lead to severe operation problems.

In order to relieve and avoid the issue of bogies covered with snow and ice in the cold regions, many countries, such as Sweden, Russia and Japan, have carried out corresponding strategies. Jemt *et al*. (2002) adopted the environmentally friendly heating propylene glycol as the material added into the removal ice equipment to improve the problem that the snow generates on the rail in the Scandinavian countries, as shown in Fig. 3. Paulukuhn *et al*. (2012) usually used water and propylene mixture in the railway to ensure that the train can withstand the snow and ice damage. However, this method couldn't be avoided for low temperature and snowy environment in Russia winter. The mixture spouts out of the spray equipment after the train deiced to reduce icing in the bogie, as illustrated in Fig. 4. Bettez *et al*. (2011) used the spraying device as the ice-removing device for the requirements of high-efficient deicing of trains running on the Joetsu railway line in Japan, seeing Fig. 5. This method solved the problem of train delays caused by the formation of snow and ice effectively. However, literatures about the cause of snow packing in the high-speed train's bogie regions are rare. To investigate the problem, in this paper the computational fluid dynamics method is used to calculate the flow characteristics in the bogie region of the train. The gas-solid two-phases flow model is adopted to simulate the movement and accumulation of snow particles.

Fig. 3. Deicing device in Sweden (Jemt *et al*. 2002).

Fig. 4. Ice melting equipment in Russian (Paulukuhn *et al*. 2012).

Fig. 5. Spraying device in Japan (Bettez *et al.* 2011).

For the wind-snow two-phases flow, Fujii *et al.* (2002) conducted research on the snow condition in Japan railways, and designed the viaduct as a measure to prevent the snow, and studied the relationship between the wind speed of snow jump and snow density and water content by experimental study. The experimental results shown that the initial density range of snow particles is 36-132 kg/m^3, and it was set to 100 kg/m^3. Tominaga *et al*. (2011a) adopted numerical simulation method to simulate the snow particles accumulation and erosion conditions, and the results were compared with the test that numerical simulation and the experimental results were in good agreement. The experiment shown that the snow particle density is 100 kg/m^3. Sang *et al*. (2012) established numerical model of snowdrift. And the mixed particle size was studied, got the influence factors of the diameter of snow particles. The paper pointed out that the diameter of the snow particles was distributed in 0-0.6mm, and was mainly concentrated in the vicinity of 0.2mm. Field measurements were carried out by Mo *et al*.(2011), and they studied the distribution of snow in the area of the house. Based on the commercial fluid calculation software FLUENT, numerical model of snowdrift was established, and the numerical simulation of the snow distributions on the roof was conducted by using a numerical model. The paper pointed out that the snow particle diameter was mainly distributed between the 0-0.4mm. Tominaga *et al*. (2011b) adopted CFD numerical simulation method to simulate the accumulation depth of the snow particles, and the wind tunnel test was used to verify the feasibility of the simulation method. Beyers *et al*. (2008) adopted numerical simulation method to simulate the process of snow particles gradually forming around the building, which would help to deal with the potential accumulation of the snow in the building design. The numerical simulation method of the snow particles in two-dimensional spaces was compared with the wind tunnel test by Sekine *et al*. (1999). And it was extended to the three-dimensional space, so it determined the feasibility of the numerical simulation of the snow particles. Cao *et al*. (2016) presented a method for simulating the icing of aircraft wings based on the Eulerian two-phases flow theory and the extended heat transfer model, and the results were verified by experiments. Gordon *et al*. (2009) studied the shape, size, velocity and density of the snow particles according to the phenomenon of the accumulation of snow in cold weather, and the physical properties of snow particles were obtained. For the breakage problem of the snow particles under high-speed wind conditions, Sato *et al*. (2008) adopted wind tunnel test to study the density of snow, and the rationality was verified in the field observation results. Zhou *et al*. (2010) adopted numerical simulation technology to simulate the phenomenon of the snow particles on the roof of the airport terminal building, and the reliability of numerical simulation technology was verified by comparing the wind tunnel test. So, we can draw a conclusion that the influence of turbulence model, wind speed and wind direction to the accumulation of snow. Beyers *et al*. (2004) adopted numerical method to simulate the condition of snow around the cube, and the experiment was carried out to verify the results.

According to the above literature review, it is easily found that using numerical simulation technology can reproduce the actual situation around the train and the railway line with a high reproducibility. Therefore, in this paper, a numerical simulation method is adopted to simulate the flow field with snow particles in the bogie regions and study the cause of snow accumulation on the bogie of a high-speed train.

2. PARTICLE MOTION EQUATIONS OF DISCRETE PHASE

The shifting snow particles in the air are always affected by the slipstream of the train, so it is necessary to understand the flow characteristics around the train firstly. The three-dimensional unsteady Reynolds-averaged Navier-Stokes equations with a RNG double-equations turbulence model is used in this paper, because it improves the accuracy in the turbulent vortex and has a higher reliability and accuracy in a wider range of flow. The governing equations can be found in the literature (Wang 2004).

Snow drifting is a kind of gas-solid two-phases flow. According to the modern multiphase flow theory, the models have been used are mainly the Euler two-fluid model, the mixed model and the Lagrange particle trajectory model (Lo 2010). Lagrange particle model is a calculation method of gas-solid two-phases flow, and its application in the snow drifting is rare. However, the model has the advantages of clear physical concept and intuitive results, including in the track experience effect and historical effect of particle. Besides, it can obtain the motion information of the particles in detail (Wang 2014). Therefore, the model is used in this paper to simulate the snow distribution in the bogie regions.

In this paper, by integrating the force balance equation of the particle, the trajectory of the discrete phase particle is predicted. Among them, the external forces acting on the particles include the aerodynamic force, gravity, buoyancy, lift force, additional mass force, Basset force, Magnus force, Saffman force, pressure gradient force, etc (Li

2006). For the snow particles in this paper, the aerodynamic force and gravity are important external forces. The effects of other forces are relatively less, so they can be ignored in the analysis (Lo 2010). The equation of motion is given in Eq. (1).

$$\frac{d\vec{u}_p}{dt} = F_D\left(\vec{u} - \vec{u}_p\right) + \frac{\vec{g}\left(\rho_p - \rho\right)}{\rho_p} \tag{1}$$

In Eq. (1), $F_D\left(\vec{u} - \vec{u}_p\right)$ is the aerodynamic force on the unit mass of particles. $\vec{u}$ is the fluid phase velocity vector. $\vec{u}_p$ is the velocity of particle phase. $F_D = \frac{18\mu}{\rho_p d_p^2}\frac{C_D \,\mathrm{Re}}{24}$. μ is the dynamic viscosity. d_p is the diameter of particles. ρ_p is the density of particles. ρ is the density of air. $\vec{g}$ is the inertia acceleration vector. Re is the relative Reynolds number, which can be expressed by the equation $\mathrm{Re} = \frac{\rho d_p \left|\vec{u}_p - \vec{u}\right|}{\mu}$. C_D is the resistance coefficient.

Particle velocity at each location on the particle tracks is obtained by the integration of Eq. (1), which can be expressed in Eq. (2).

$$\frac{d\vec{x}}{dt} = \vec{u}_p \tag{2}$$

In Eq. (2), $\vec{x}$ is particle displacement vector. t is the time. The trajectory of the particle is obtained by the integration on the discrete time step gradually, and the trajectory of the particle can be obtained by the integration of Eq. (2).

3. THE WIND TUNNEL EXPERIMENT VALIDATION

In order to verify the correctness of the numerical results, the wind tunnel experiment was carried out, and the numerical simulation results were compared with the wind tunnel test results. In the wind tunnel experiment, the original model was used, and the numerical model of the bogie was consistent with the model used in the wind tunnel test, as shown in Fig. 6.

In order to avoid the interference of the flow of the end of the train body to the bogie region, the train body was simplified to 30-degrees inclined end surface to achieve the diversion effect, the vehicle height is 0.7m, the train body length is 3.6m, as shown in Fig. 7.

The experiment was carried out in the National Engineering Laboratory of High-speed Railway Construction Technology, and the size of the high-speed section is 3m×3m×15m. The fixed floor was used to reduce the flow field interference of the bogie by the boundary layer thickness, and the distance between the fixed floor and the tunnel ground is 1m. In addition, to simulate the flow field at the bottom of the train, the 1:2 rail model was installed on the fixed floor, as shown in Fig. 8. In the numerical simulation domain, the fixed floor and rail models were added, and the influence of the bottom floor bracket on the flow field of the bogie was ignored, as shown in Fig. 9.

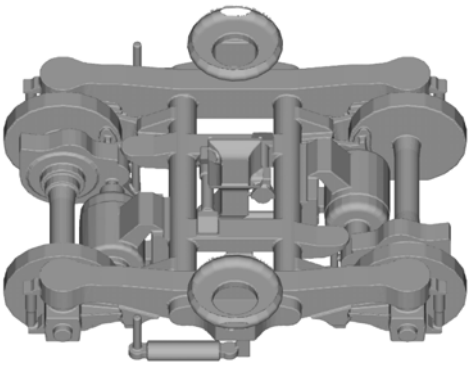

Fig. 6. Bogie model.

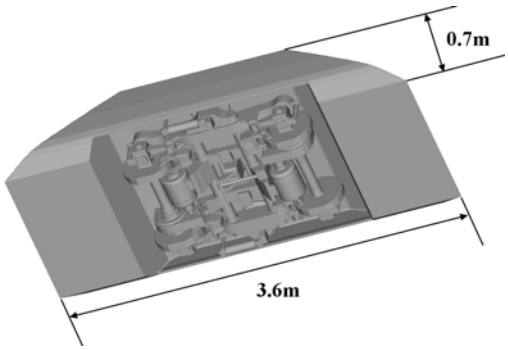

Fig. 7. Train model.

Fig. 8. Experimental set-up.

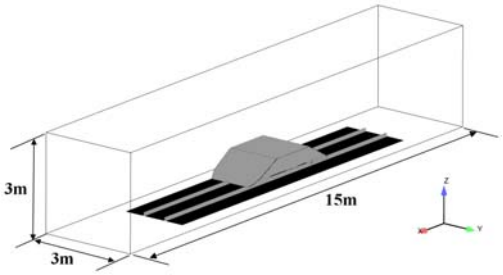

Fig. 9. Numerical domain.

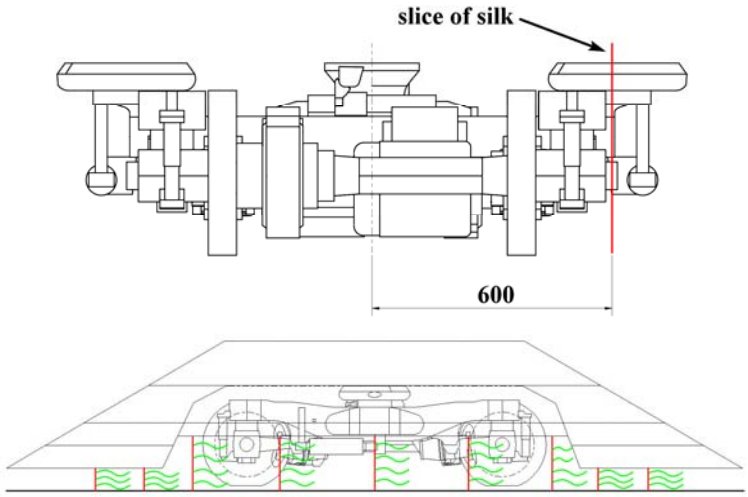

Fig. 10. Position of tufts.

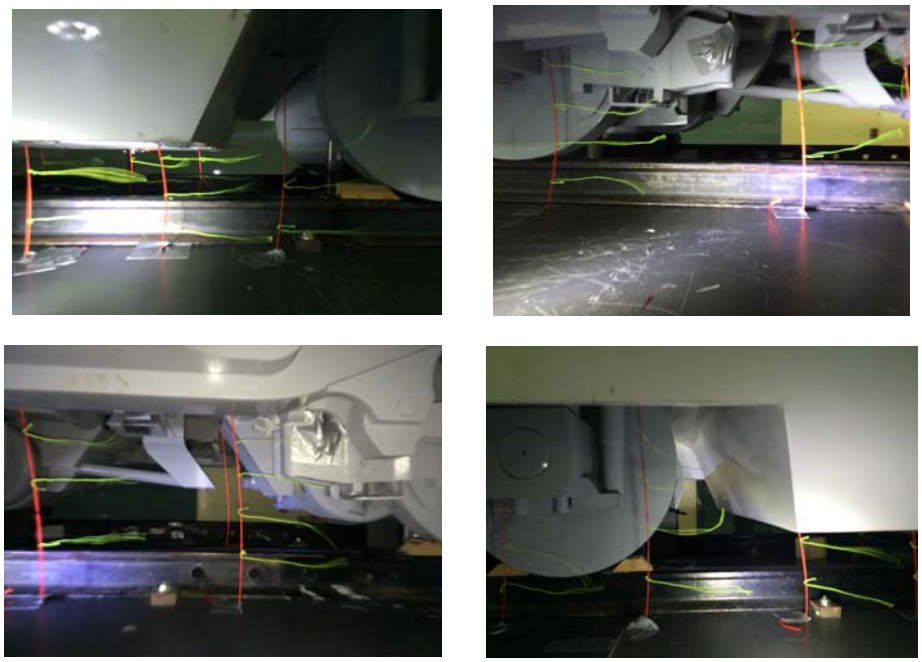

Fig. 11. Tuft flow in wind tunnel tests.

The wind speed in wind tunnel experiment and numerical simulation is 35m/s, and the Reynolds number calculated through wind speed and characteristic length is 1.67 $\times 10^6$, which meets the requirements of Reynolds number in wind tunnel tests (CEN EN 2009). To ensure the reliability of the experimental data, the TFI Cobra Probe 270 is used to measure the velocity of the flow field. A high-frequency pressure-scanning valve is used to collect the pressure, and the light-green silks with the high-speed photography are selected in order to ensure the accuracy of the experimental results. The simulation is carried out in Fluent software, and the flow field of the bogie is simulated by using the k-epsilon turbulence model.

As shown in Fig. 10, the tufts are arranged on the longitudinal section outside the track. And the streamlines in the bogie region of the wind tunnel experiment and the numerical simulation are respectively shown in Figs. 11 and 12.

It can be concluded from Figs. 11 and 12, in the bottom region of the original model, the streamlines in the wind tunnel experiment and the numerical simulation are relatively stable in most of area. However, the streamlines close to the wheels, brakes, electromotors and other parts are upwards. And, the vortices are formed at the back end of the bogie. Overall, the flow directions in numerical simulations are in good agreement with those tuft directions in the wind tunnel tests. The numerical method is reliable enough to obtain the accurate numerical simulation results.

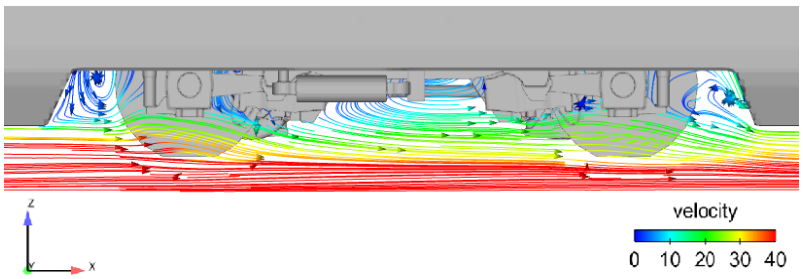

Fig. 12. Streamlines in the simulation.

4. COMPUTATIONAL DETAILS FOR CFD ANALYSIS

4.1 Geometry and Computational Model

The train is a slender body with the length of 200m that consists of eight vehicles. Each vehicle has 2 bogies. To simulate this wind/snow two-phase flow, hundreds of millions of particles are needed to be released into the region, and each particle has a corresponding equation. As each time step is taken, the number of equations increases gradually. It is very hard to simulate the snow packing on each bogie based on the discrete phase model, which needs massive computational resources. Meanwhile, the bogies with cavities are the representative cases in the train under-body regions. Therefore, in this stage we attempted to explore the flow characteristics around a bogie with part of the train body and estimate the general situation of the snow and ice covering on the bogie. So, in the calculation, only one bogie area is chosen as the research object at first. In the future, more bogie regions will be taken into account.

In order to simulate the flow field structures below the bottom of the train body, the rail model is added into the geometry. To ensure the full development of the flow field and avoid the influence of boundary conditions on the flow structures around the bogie, a computational domain with 60m long, 20m wide and 20m high is established. The distance between the train and inlet is 15m. And, the distances between the bogie center and the front and back end of the train are both 8.75m, the height of the bogie is 1.02m and the length is 3.43m. These distances are reasonable for the flow field of the bogie to avoiding disturbances. The model is put in the middle along the Y axis direction, as shown in Fig. 13. The blocking ratio of the computational domain is 2.8%, less than 5%.

There are many types of high-speed trains in our country, such as CRH1, CRH2, CRH3 and CRH5. These four types of trains all use the bottom-cover structures, so the bogie cut out seems to be a cavity. In this paper, the calculated models also come from CRH2, including one with inclined plate and the other with straight plate, as shown in Fig. 14. According to the traction effect, there are power bogies and the non-powered bogies. Actually, from the field investigation, it is shown that the power bogies are covered with more snow and ice, so this bogie is chosen as the research object. In this paper, the train body and bogie are simplified, and the gaps between the moving parts (e.g. wheels and tracks) are adjusted to facilitate the grid generation.

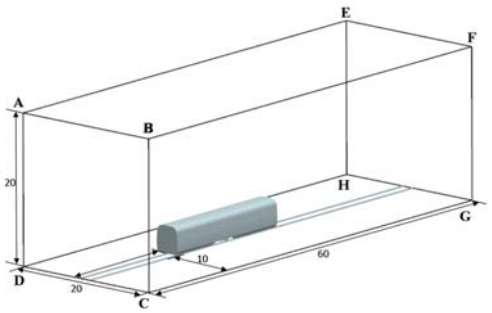

Fig. 13. Computational domain (unit:m).

There are so many heat sources on the bogie such as electromotors, brakes and so on. In the calculation, much more attention should be paid on these to investigate the flow field in the bogie region. Fig. 15 shows the locations of the main parts on the bogie.

The OpenFOAM mesh generator package-SnappyHexMesh was applied to generate the hexahedral dominated mesh. Figs. 16 and 17 show the surface grids of the bogie and the section views of the grids around the bogie and train body with inclined end plate respectively.

Based on the discrete phase model, it is not allowed to use a scaled model to simulate the snow particles travel in the computational domain, so in the paper a 1:1 model is used to study the flow characteristics around the train body with a single bogie. To obtain precise flow structures between the train body and the ground, the grids in these regions are refined. However, the grids around the train are relatively coarse. When the velocity is 55.56m/s, the y+ values on the bogie are roughly in the range from 30 to 300 to ensure the use of wall function in k-epsilon turbulence model (ANSYS Inc. 2014). The number of volume grids is about 1.4 million, and 6 boundary layers are uniformly distributed around the train and bogie.

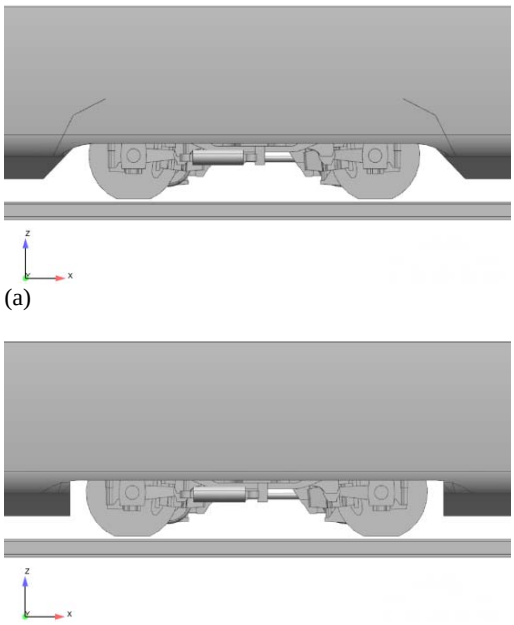

(a)

(b)

Fig. 14. Calculated train models: (a) Inclined end plate model, (b) Vertical end plate model.

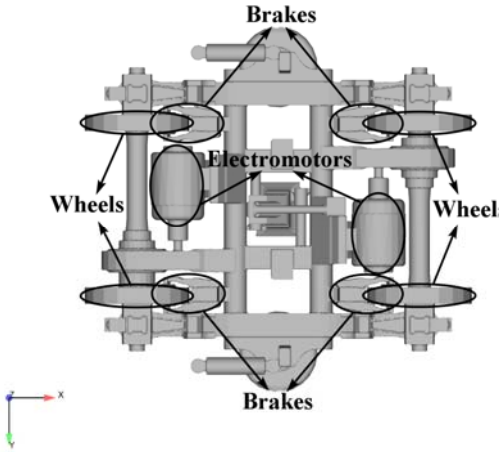

Fig. 15. Main parts on the bogie.

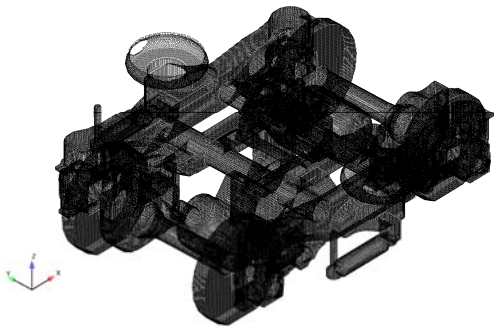

Fig. 16. Bogie surface grids.

4.2 Boundary Conditions and Parameter Settings

The Fluent that is a commercial CFD solver is used. And the SIMPLEC algorithm is used in the computational method to couple the pressure and the velocity field. Unsteady state calculation is used to obtain the unsteady flow field. The density of the snow particles is 100kg/m^3, and the particle diameter is uniformly distributed as 0.2 mm. The train speed is 200km/h. The time step is 0.001s that gives the courant number is roughly from 0 to 11.85, and mainly concentrates between 0 and 1 in the calculation. Therefore, the time step meets the requirement. When t = 2.00 s, the flow passes through the domain one time, and the wind/snow flow field in the bogie becomes relatively stable and fully developed. Therefore, taken into account the scale of calculation, the calculated time is set to 2.00 s with 2000 time steps For the snow particles in the bogie region, most of them will be captured by the bogie, and some will be escaped. In this paper, taking the worst condition into account, all of these snow particles will be captured on the bogie. The specific boundary conditions are shown in Table 1.

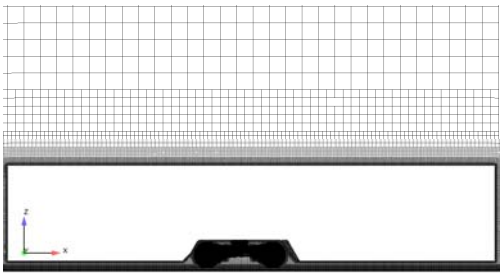

(a)

(b)

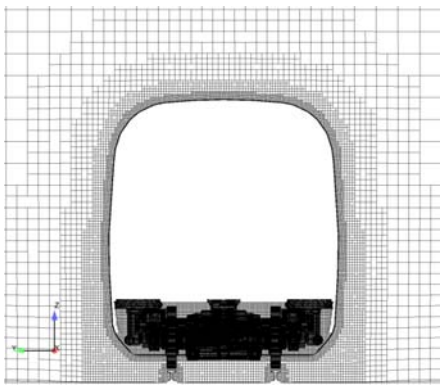

Fig. 17. Grids around the bogie and train body with inclined end plate:(a) y direction, (b) x direction.

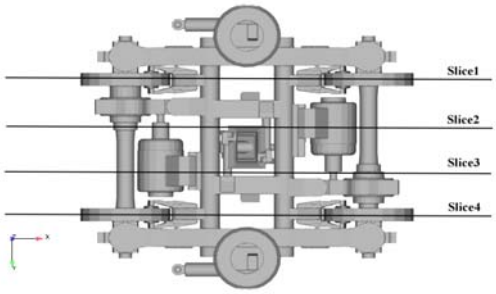

Fig. 18. Slices in the bogie region parallel to the X axis direction.

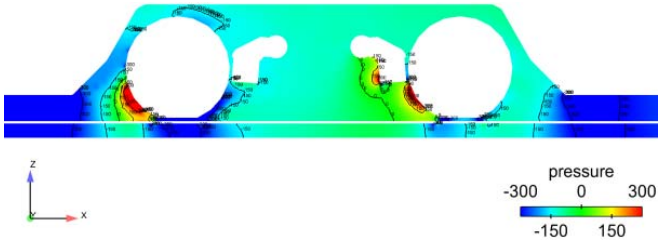

(a)

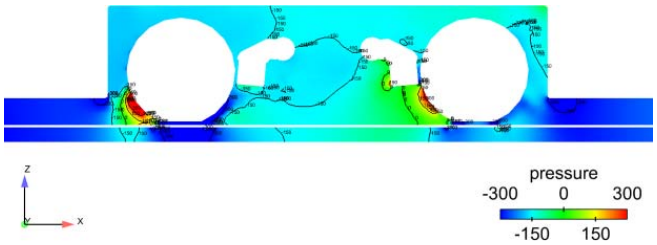

(b)

Fig. 19. Pressure distributions at the position of slice 1 in the bogie region: (a) Case1, (b) Case2.

(a)

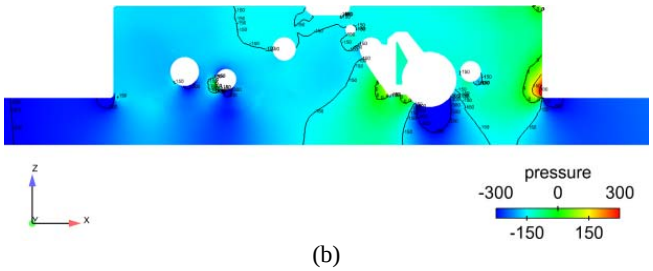

(b)

Fig. 20. Pressure distributions at the position of slice 2 in the bogie region: (a) Case1, (b) Case2.

Table 1 Boundary conditions for CFD analysis

Domain boundary	Boundary condition	Parameter setting
ABCD	Velocity inlet	X=55.56m/s, Escape condition
BCGF, ADHE, ABFE	Non-slip wall	Escape conditions
EFGH	Pressure outlet	Escape condition
CGHD	Slip wall	X=55.56m/s, Escape condition
train, wheels	Non-slip wall	Reflection conditions
bogie, electromotors, plates, brakes	Non-slip wall	Trap conditions

5. Analysis Of Snow Packing On The Bogies

Based on the two original models, the pressure fields and streamlines around the bogies are investigated. After that, the movement of snow particles in the bogie regions and the snow accumulation on the bogies are analyzed.

The slices parallel to the X axis direction are used, as shown in Fig. 18. The slices 1 and 4 are cut on the wheels and the brakes of the bogie, and the slices 2 and 3 are focused on the electromotors of the bogie. And, in the following analysis, we will simplify the inclined end plate model to Case1, and the vertical end plate model to Case2.

5.1 Pressure Distributions Around Bogies

In order to investigate the pressure distributions

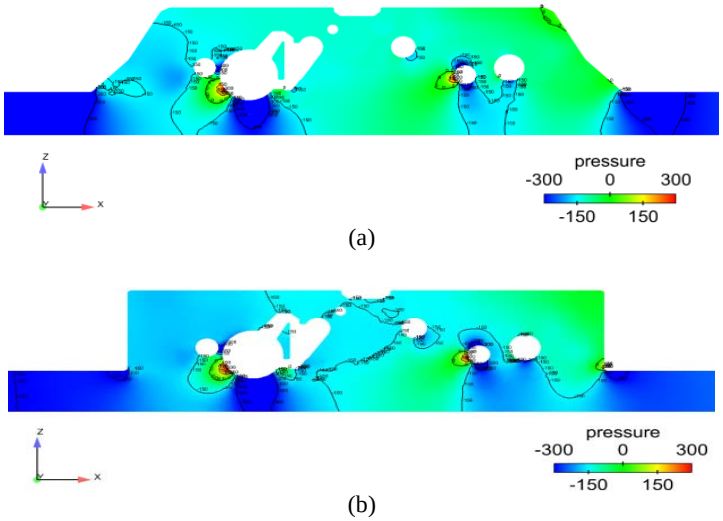

Fig. 21. Pressure distributions at the position of slice 3 in the bogie region:(a) Case1, (b) Case2.

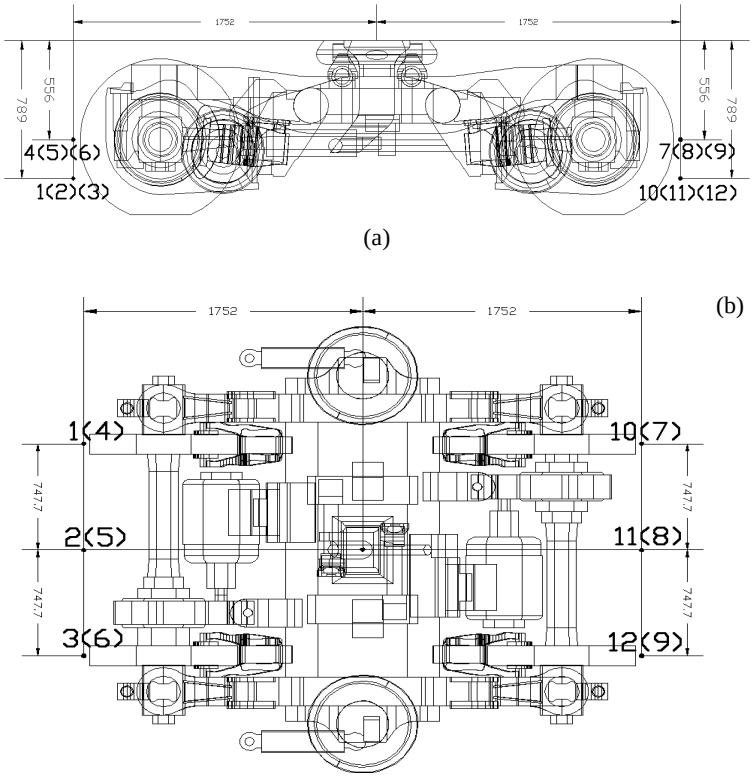

Fig. 22. Set up of pressure monitoring points:
(a) Side view, (b) Top view.

around the bogies of two different models, the pressure contours on the slices are shown in Figs., 19, 20 and 21. The slices 1, 2 and 3 are chosen to make a comparison.

By observing the pressure distributions of the two models, the pressure distributions around the wheels, brakes and electromotors can be seen clearly. There is negative pressure in the region below the train bottom that is away from the bogie. On the windward sides of the wheels, brakes, electromotors and other prominent parts, there is positive pressure due to the impact of the flow. Except that, all sides are suffered negative pressure.

On the same region in the two models, some visible differences can be seen clearly. To know accurately these, some pressure monitoring points around the bogies are set up, as shown in Fig. 22, and the pressure values can be found in Table 2. Among them, these points are distributed around the bogie at different heights and different lateral positions, and the Pcase1/Pcase2 (%) is the ratio between Case1 and Case2.

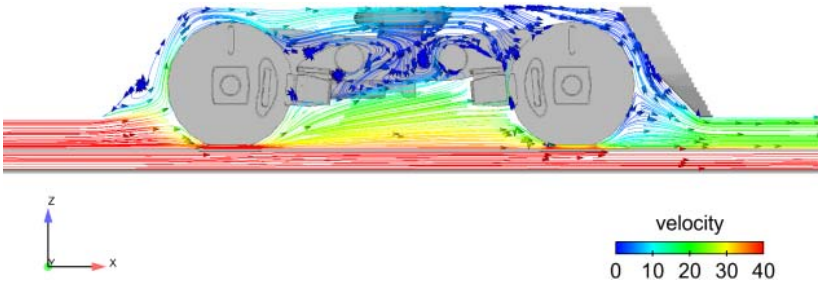

(a)

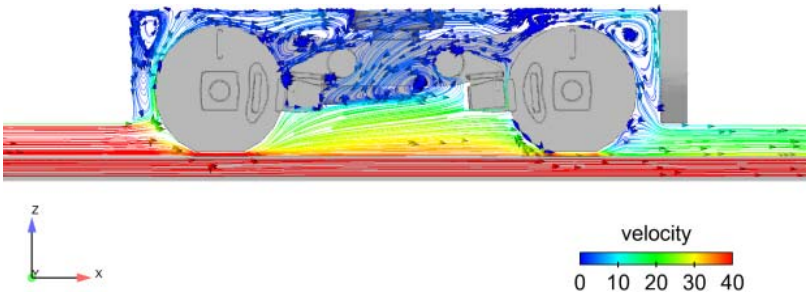

(b)

Fig. 23. Streamlines on slice 1 in the bogie region: (a) Case1, (b) Case2.

Table 2 Pressure of monitoring points in two models

models / points	Case1 (pa)	Case2 (pa)	Pcase1/Pcase2 (%)
1	433.1	257.9	167.9
2	-184.5	-163.1	113.1
3	421.7	225.1	187.3
4	-196.4	-176.4	111.3
5	-194.5	-172.6	112.7
6	-201.9	-187.8	107.5
7	-149.8	-228.9	65.4
8	-74.2	-93.3	79.5
9	-137.1	-234.5	58.5
10	-134.8	-156.7	86.0
11	-70.5	-97.7	72.2
12	-125.6	-162.2	77.4

Concerning the pressure at these monitoring points, in the front region of the bogie, for case 1 it will generate higher positive pressure and lower negative pressure, compared with that in Case2, which seems that in this region the pressure changes so quickly. After that between two models there are large pressure differences, especially at these monitoring points, such as the points 1 and 3, which are close to the ballast and wheels. However, in the end region of the bogie, the pressure shows smoother than in the front of both models with negative values, and for Case1 this phenomena is much more obvious. Consequently, there are still some certain pressure differences between the two models. Based on the analysis, it can be found that in the front region using the Case2 model with a vertical end plate and in the end region using the Case1 model with an inclined end plate will obtain a slower changing pressure environment.

Obviously, the pressure difference in the bogie region will lead to the change of flow direction, as the flow comes into the bogie region from the bottom of the train. The flow impacts on the wheels, brakes, electromotors and other parts, seeing Figs. 23, 24 and 25. Sometimes, it even travels over the top of the bogie, as shown in Figs. 23, 24 and 25.

5.2 Streamlines in Bogie Regions

To further understand the flow direction in the bogie region, according to the slices in Fig. 11, some streamlines colored with velocity are draw on these planes, as shown in Fig. 23, 24 and 25.

From the streamlines of the two models, it can be seen, below the bottom of the train, the flow direction changes coming into the bogie region. It raises an angle between the horizontal plane and moves towards the topside, generating lots of vortex with low speed. Part of flow travels through the bogie region, and then it is blocked at the end of the plate causing inverse flow. Due to the different structures in the two train bodies, streamlines around the bogies seem to be not the same. For Case1 the inclined plate contributes to a higher raising angle of the flow that would affect the flow structure in the front region of the bogie, leading to less vortex generation but higher velocity, as shown in Figs. 23-25. In the end, the inclined plate will

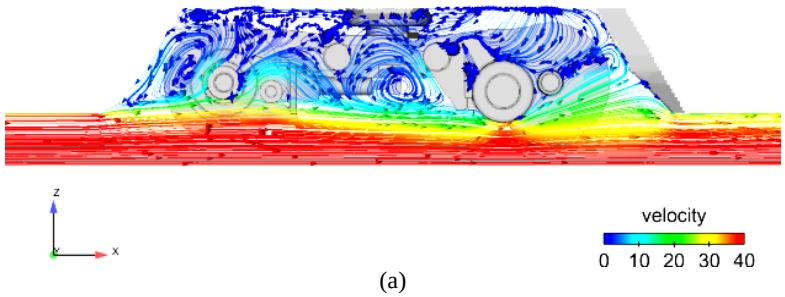

(a)

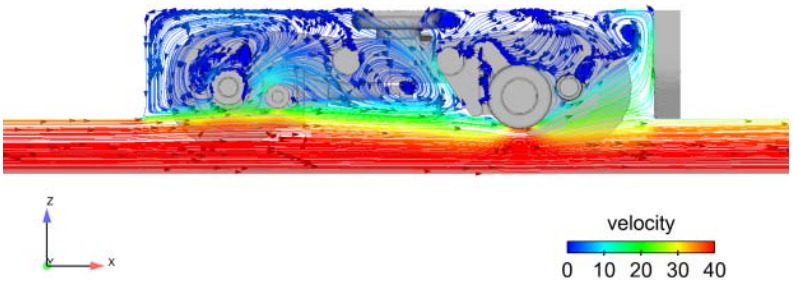

(b)

Fig. 24. Streamlines on slice 2 in the bogie region: (a) Case1, (b) Case2.

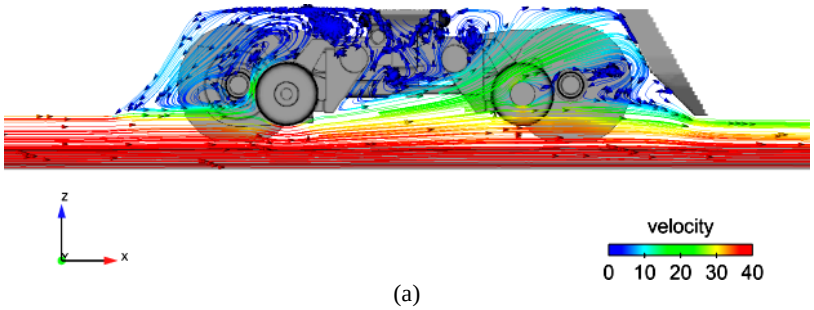

(a)

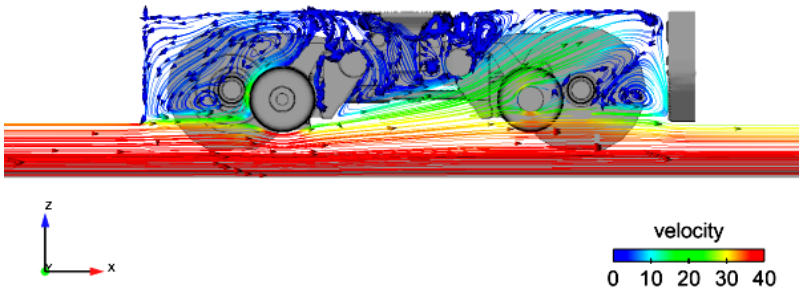

(b)

Fig. 25. Streamlines on slice 3 in the bogie region: (a) Case1, (b) Case2.

help the incoming flow travel out. However, for the geometry of the bogie is very complex, the flow structure in the bogie region will be more turbulent accompanying much incoming flow. For Case2, large vortices are generated at the corners, and the vertical end plate blocks the way of the incoming flow, causing some vortices, seeing Figs. 23-25. Although the incoming flow is less, the flow structure in the bogie region is also very turbulent. Fortunately, the velocity above the bogie is very low. In summary, at the front end, the Case2 is more effective than the Case1 to reduce the rise in air flow, and, at the back end, the Case1 is more effective than Case2 in avoiding backflow. All these complex geometries and turbulent vortices will help the snow accumulate on the bogie, as shown in Figs. 19 and 20.

5.3 Movement of Snow Particles in the Bogie Regions

The discrete phase model is used to study the movement of snow particles in the bogie regions at 6 different time, these are t= 0.10s, 0.12s, 0.16s, 0.20s, 0.40s, 2.00s, as shown in Fig. 26.

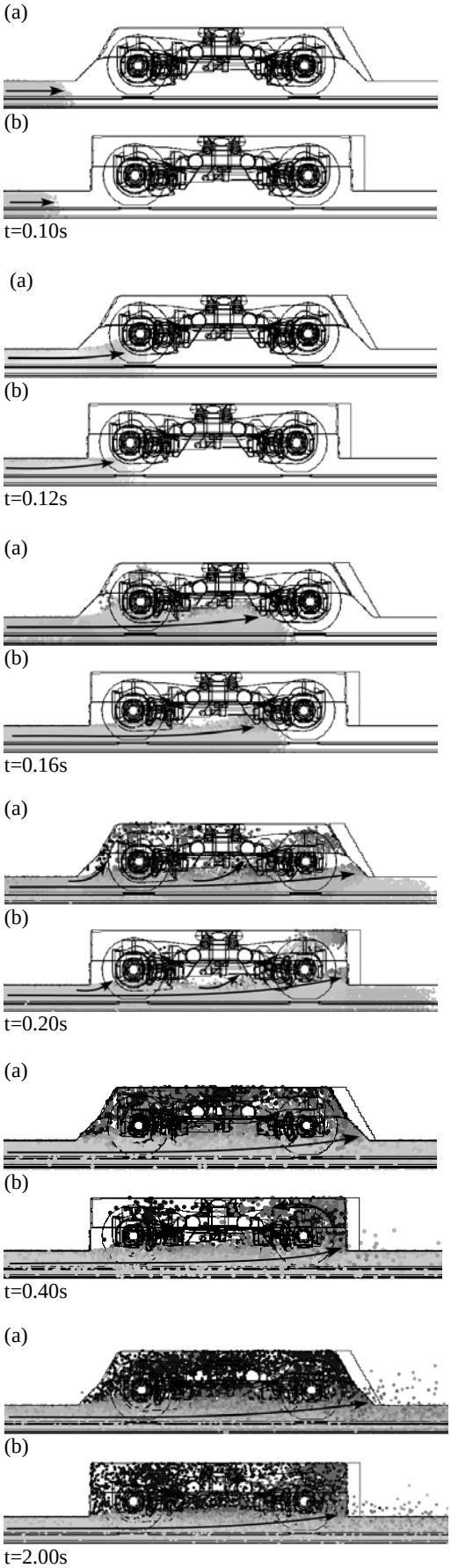

Fig. 26. Movement of snow particles in the bogie regions: (a) Case1, (b) Case2.

When t = 0.10s, the snow particles begin to move into the front of the bogie. After 0.12s, these snow particles are impacting on the front wheels and axles. When the time is up to 0.16s, the snow particles enter the central area of the bogie and have effects on the front half structure of the bogie, but these particles are concentrated below the bottom of the train. When the time arrives 0.20s, the snow particles go through the whole area of the bogie. The particles are subjected to the gravity, so the trajectory deflects to ground, and then there will be free snow particles get into the interior of the bogie. When the time lasts 2.00s, the snow particles are fully filled in the bogie regions, which can be seen as a relative stable wind/snow particles environment in the bogie region.

Compared with the streamlines and the movement of snow particles in Section 4.2 and Section 4.3, it can be found that the results are not exactly consistent with the trajectory of the snow particles and the streamlines. In the front of the bogie region, the snow particles are followed the flow direction, but except this the trajectory of the particles and the flow are not in the similar directions due to the complex flow structures and the inertia of mass particles. Therefore, the snow particles are always packing around the point where the velocity direction changes a lot, such as the windward side of the bogie region.

On the other hand, for Case1 a higher raising angle of the flow lifts the snow particles, which move towards the end with the time, to the top of the bogie in the front region. After 0.2s, the snow particles are almost full filled in the bogie region, while for Case2 some particles that have the trend toward shifting with the air just accumulate in the end region of the bogie where the flow is blocked, as shown in Fig. 26. 2s later, both of the two cases are full with snow particles, especially in Case1. To understand the snow accumulation on the bogies and obtain some quantitative results, as shown in Section 4.4, the snow accumulation in the bogie region is investigated.

5.4 Snow Accumulation in the Bogie Region

After 2.00s, massive snow particles are in the bogie region, so it is very suitable to present the snow packing on the bogies, as shown in Figs. 27 and 28. In order to distinguish the main parts with snow accumulation in the bogie regions of two models, two different snow concentrations are used. When the snow concentration is more than 1×10^{-12}kg/m^3, the snow colored with velocity can be seen as shown in Fig. 27. At this snow concentration, it is found that most of the bogie is covered with snow. After that, when the snow concentration increases up to 5×10^{-10}kg/m^3, the snow particles are packing in several areas, as shown in Fig. 28.

In Fig. 27, compared with the bottom-up view and the overhead view, massive snow particles are covered on the bogies of the two models, especially on the bottom of the bogies. There is a lot of snow packing on the bogie's windward side, and much less snow is on the leeward side. According to the

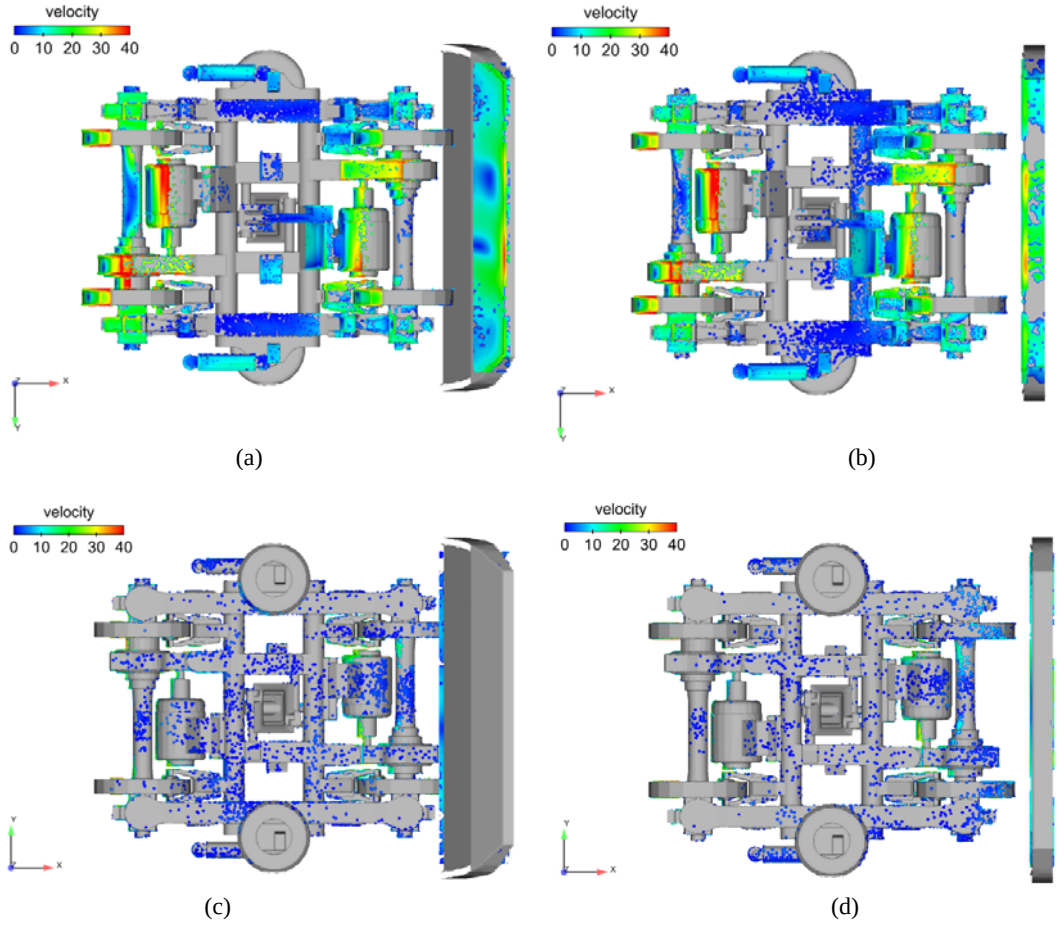

Fig. 27. Widely accumulation of bogie region: Bottom-up view of Case1, (b) Bottom-up view of Case2, (c) Overhead view of Case1, (d) Overhead view of Case2.

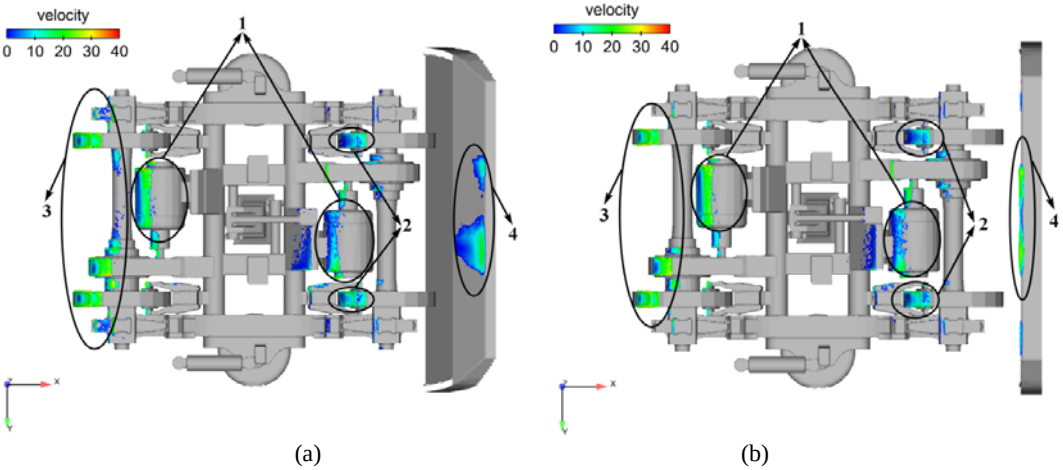

Fig. 28. Centered accumulation of bogie region:(a) Bottom-up view of Case1, (b) Bottom-up view of Case2（1 - The electromotors; 2 - The brakes; 3 - The wheels; 4 - The deflectors）.

Figures 27 and 28, the snow accumulation is mainly concentrated on the bottom-windward region of the wheels, brakes, electromotors, plates and so on. However, the snow is packing less on the upper side and the leeward side.

To observe the accumulation of the snow in the bogie region, the snow concentration of 1×10-12kg/m^3 is chosen, seeing Figs. 29, 30 and 31 colored with velocity.

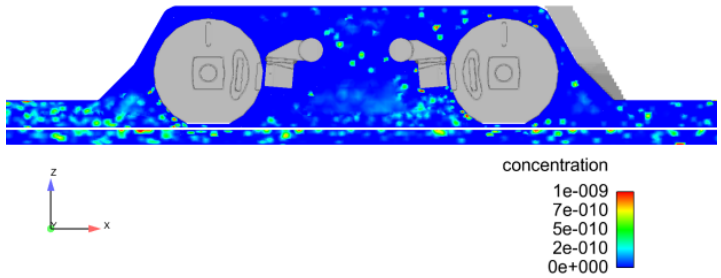

(a)

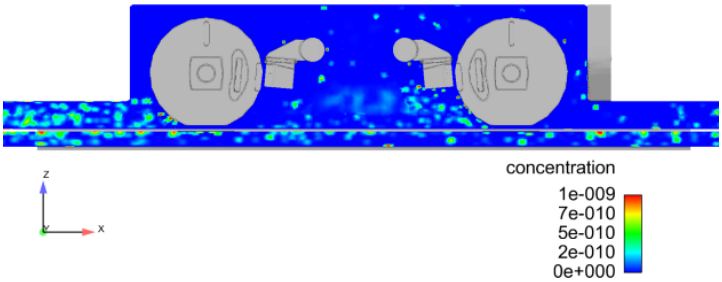

(b)

Fig. 29. Snow concentration on slice 1 in the bogie region: (a) Case1, (b) Case2.

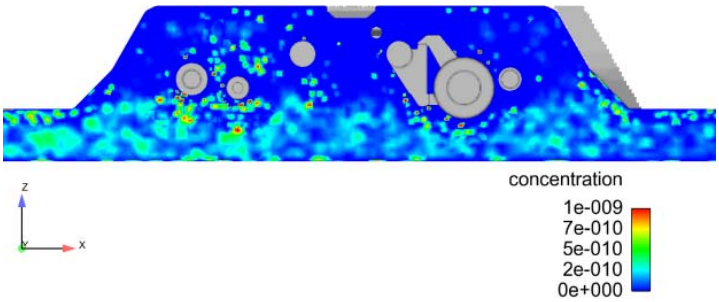

(a)

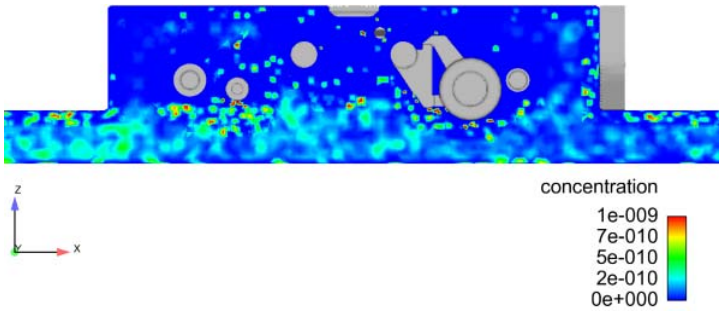

(b)

Fig. 30. Snow concentration on slice 2 in the bogie region: (a) Case1, (b) Case2.

In Figs. 29-31, the snow concentration is a little larger around the wheels, brakes and electromotors in the bogie region of two models, which is favorable for the snow to melt, causing severe ice problems. And there is much more snow packing on the bottom of the bogies where is directly impacted by the flow than on the top.

Work has been done to know how many snow particles the bogies capture on the bogies, including the wheels, brakes, electromotors, bogie frames and back-plates, some data are presented in Tables 3 and 4.

The number of snow particles on the wheels, brakes, electromotors and bogie frames in Case1 are greater than Case2. However, the numbers on the back-plate of Case1 are less than Case2, which indicates that the inclined plate in the front region takes similar effect on the vertical plate in the end region after the enough simulation time. That it is to say, in the front, using the vertical plate less incoming flow with snow particles will come into

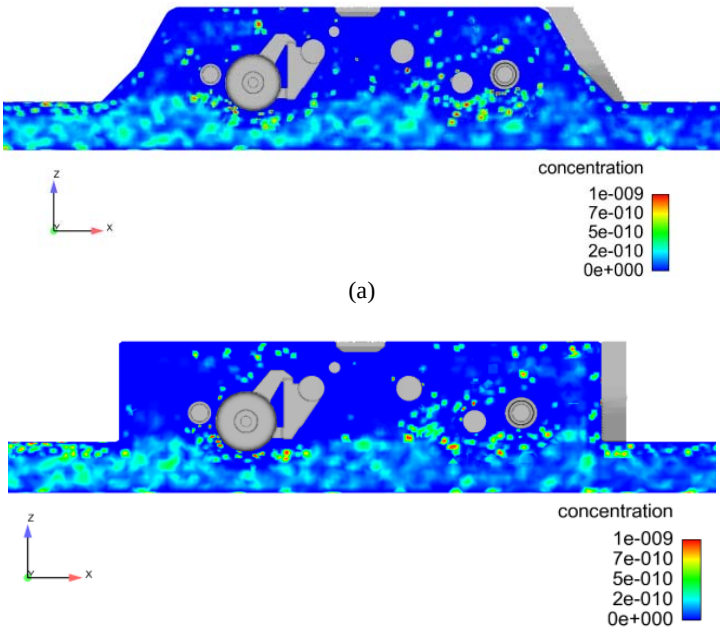

Fig. 31. Snow concentration on slice 3 in the bogie region: (a) Case1, (b) Case2

Table 3 Number of captured snow particles on the bogies

Models / Parts	Case1	Case2	Ccase1/Ccase2(%)
Wheels	57605	40244	143.1
Brakes	16134	12353	130.6
Electromotors	32848	30874	106.4
Bogie frames	88485	46299	191.1
Sum up	195072	129770	150.3

Table 4 Number of captured snow particles on the back-plates

Models / Parts	Case1	Case2	Ccase1/Ccase2 (%)
Back-plates	23806	30646	77.7

the bogie region, while employing the inclined plate at the end the flow with snow particles will be easily travel out.

6. CONCLUSIONS

It is a significant challenge for the high-speed train to run in the winter, especially in a harsh and unfavorable environment. Massive snow on the ground and ballast will whirl around the moving train, which could lead to severe snow accumulation on the bogies. In this paper the CFD technology with a gas-solid two-phase flow model was used to investigate the snow shifting and packing in the bogie regions of two models, including an inclined end plate model and a vertical end plate model. And, the numerical simulation is verified by the wind tunnel test.

Firstly, pressure and streamlines on the slices along the X axis direction were studied, which shows that when the air incoming from the bottom flows into the bogie regions will obtain a raising angle and impact on the wheels, brakes, electromotors and other parts of bogie regions. Besides this, the end plate in the bogie region blocks the air, and makes the flow structure more turbulent, which contributes to the snow packing on the bogie.

Then, to know the entranceway of shifting snow particles into the bogie regions of two different models, the movement of snow particles was

monitored herein. In front of the bogies the streamlines of the air and the particle path lines are basically the same. For the inclined plate model the particles would be easier move towards the top of the bogie in the front. However, due to the inertia of mass particles, the following characteristics of the snow particles with the air are not obvious in the bogie leeward side.

Finally, the snow accumulation in the bogie regions was presented. It indicates that the main parts of the snow accumulation are the bottom and the windward sides. Different structures of the end plates will affect the snow accumulation in the bogie regions. In the front the vertical end plate of Case2 have a better optimization effect, while at the end the inclined Case1 will be more effective. All of these will provide the basis for the anti-snow investigation of high-speed train's bogies in the future.

This demonstrates the applicability of CFD modeling in providing useful information for train safety in heavy snow. However, it is not fully exploited as the snow drifts around the bogie region. Validation and optimizations on the bogies are necessary in the next work.

ACKNOWLEDGEMENTS

The authors acknowledge the computing resources provided by the High-speed Train Research Center of Central South University, China.

This work was supported by the National Key Research and Development Program of China (Grant No. 2016YFB1200403), the Project of Innovation-driven Plan in Central South University (Grant No. 2015CX003), the Strategic Leading Science and Technology Project of Central South University (ZLXD2017002) and the National Science Foundation of China (Grant Nos. U1334205 and U1534210).

REFERENCES

Bettez, M. and *et al.* (2011). *Winter technologies for high speed rail*. Norwegian University of Science and Technology, Trondheim, Norway.

Beyers, J. H. M., P. A. Sundsbø and T. M. Harms (2004). Numerical simulation of three-dimensional, transient snow drifting around a cube. *Journal of Wind Engineering and Industrial Aerodynamics* 92(9):725-747.

Beyers, M. and B. Waechter (2008). Modeling transient snowdrift development around complex three-dimensional structures. *Journal of Wind Engineering and Industrial Aerodynamics* 96(10), 1603-1615.

Cao, Y., J. Huang and Y. Jun (2016). Numerical simulation of three-dimensional ice accretion on an aircraft wing. *International Journal of Heat and Mass Transfer* 92,34-54.

CEN European Standard, (2009). *Railway Applications- Aerodynamics. Part 4: Requirements and Test Procedures for Aerodynamics on Open Track.* CEN EN 14067-4.

Fluent Inc. *FLUENT User's Guide,* 2014.

Fujii, T. and K. Kawashima (2002). Preventive Measures against Snow for High-Speed Train Operation in Japan. *International Conference on Cold Regions Engineering*, Alaska, United States, 448-459.

Gordon, M., S. Savelyev and P. A. Taylor (2009). Measurements of blowing snow, Part II: Mass and number density profiles and saltation height at Franklin Bay, NWT, Canada. *Cold Regions Science and Technology* 55(1), 75-85.

Gordon, M., S. Savelyev and P. A. Taylor (2009). Measurements of blowing snow, Part I: Particle shape, size distribution, velocity, and number flux at Churchill, Manitoba, Canada. *Cold Regions Science and Technology* 55(1), 63-74.

Jemt, T. and *et al.* (2009). De-icing solution. International Railway Journal 49(1):24-25.

Kloow, L. and *et al.* (2006, February). High-speed train operation in winter climate. *Transrail Publication BVF* 5(2).

Lo, S. and *et al.* (2010). Computational Techniques for Multi-Phase Flows. *Chemical Engineering* 117(7), 8-9.

Mo, M. and *et al.* (2011). *Numerical simulation and experimental study on snow distribution on typical roofs.* Harbin Technical University, Harbin, China.

Ni, J. and Z. Li (2006). *Wind blowing sand two-phase flow theory and its application*. Beijing Science Press, Beijing, China.

Paulukuhn, L and X. Wu (2012). The Low Temperatures Technology Concepts and Operational Experience in Russian High Speed Train Velaro RUS. *Foreign Rolling Stock* 49(3), 16-19.

Sang, J. and *et al.* (2012). *Numerical simulation of blowing snow with mixed diameter*. Lanzhou University, Lanzhou, China.

Sato, T., K. Kosugi, S. Mochizuki and M. Nemoto (2008). Wind speed dependences of fracture and accumulation of snowflakes on snow surface. *Cold Regions Science and Technology* 51(2):229-239.

Serine, A., M. Shimura, A. Maruoka and H. Hirano (1999). The numerical simulation of snowdrift around a building. *International Journal of Computational Fluid Dynamics* 12(3-4):249-255.

Tominaga, Y., A. Mochida and T. Okaze (2011a). Development of a system for predicting snow distribution in built-up environments: Combining a mesoscale meteorological model and a CFD model. *Journal of Wind*

Engineering and Industrial Aerodynamics 99(4), 460-468.

Tominaga, Y., T. Okaze and A. Mochida (2011b). CFD modeling of snowdrift around a building: An overview of models and evaluation of a new approach. *Building and environment* 46(4), 899-910.

Wang, F. and *et al.* (2004). *Dynamic analysis of computation fluent: Theory and its application of CFD software.* Tsinghua University Press, Beijing, China.

Wang, W., H. Liao and M. Li (2014). Lagrange stochastic model to simulate snow distribution in roofs. *Chinese Journal of Applied Mechanics* 31(3), 428-434.

Zhou, X. and X. Li (2010). Simulation of Snow Drifting on Roof Surface of Terminal Building of an Airport. *Disaster Advances* 3(1), 42-50.